Micromechanical modelling of sulphate corrosion in concrete: influence of ettringite forming reaction

M. Basista [*]   W. Weglewski [†]

Abstract

Two micromechanical models are developed to simulate the expansion of cementitious composites exposed to external sulphate attack. The difference between the two models lies in the form of chemical reaction of the ettringite formation (through-solution vs. topochemical). In both models the Fick's second law with reaction term is assumed to govern the transport of the sulphate ions. The Eshelby solution and the equivalent inclusion method are used to determine the eigenstrain of the expanding ettringite crystals in microcracked hardened cement paste. The degradation of transport properties is studied in the effective medium and the percolation regime. An initial-boundary value problem (2D) of expansion of a mortar specimen immersed in a sodium sulphate solution is solved and compared with available test data. The obtained results indicate that the topochemical mechanism is the one capable of producing the experimentally observed amount of expansion.

Keywords: chemo-damage, sulphate attack, topochemical reaction, through-solution reaction, ettringite, micromechanics, microcracking, percolation.

1   Introduction

The durability of concrete structures is affected by many environmental factors, the sulphate corrosion being one of the most frequent and detrimental processes. The sulphate ions if contained in the ground waters may diffuse

---

[*]Institute of Fundamental Technological Research Polish Academy of Sciences, Swietokrzyska 21, 00-049 Warsaw, Poland, e-mail: mbasista@ippt.gov.pl

[†]Institute of Fundamental Technological Research Polish Academy of Sciences, Swietokrzyska 21, 00-049 Warsaw, Poland

through the capillary pores of concrete due to the concentration gradient and react with unhydrated components of the hardened cement paste. In consequence, these chemical reactions may lead to expansive reaction products such as *ettringite*. In turn, the ettringite may cause the overall expansion of a structural element and its extensive damage progressing from the outer surface towards the specimen inner core (e.g. Skalny *et al.*, 2002). This process may result in a gradual loss of concrete strength accompanied by surface spalling and exfoliation (Biczok, 1972).

The migration of sulphate ions by diffusion and the mechanisms of concrete expansion due to sulphate attack on Portland cement concrete have been a subject of extensive experimental, analytical and numerical investigations in the past, e.g. Mehta (1983), Ouyang et al. (1988), Odler and Gasser (1988), Cohen and Bentur (1988), Moukwa (1990), Ping and Beaudoin (1992), Snyder and Clifton (1995), Gospodinov et al. (1996), Brown and Taylor (1999), Samson et al. (2000), Marchand, (2001), Brown and Hooton (2002), Mironova et al. (2002). The vast body of specialized literature on sulphate attack comprises also comprehensive state-of-the-art papers, e.g. Cohen (1983a), Cohen and Mather (1991), Mehta (2000), Santhanam et al. (2001), monographs and special thematic volumes, e.g. Biczok (1972), Soroka (1980), Mehta and Monteiro (1993), Lea (1998), Marchand and Skalny (1999), Skalny et al. (2002).

As far as the modelling of suphate induced deformation and damage is concerned some continuum mechanics models have been proposed which addressed the chemo-damage coupling within phenomenological settings, e.g. Saetta et al. (1993, 1998), Tixier and Mobasher (2003), Kuhn et al. (2004). However, except for the pioneering effort of Krajcinovic et al. (1992), a comprehensive micromechanical model of sulphate corrosion damage in concrete is still lacking.

An interesting scientific dispute becomes evident when reviewing the existing literature on the sulphate attack on concrete. For over 40 years the experts in this field were not able to resolve a controversy about the chemical mechanism in which the expansive ettringite is formed. Some authors claimed that expansive ettringite is formed in a two-stage topochemical reaction between sulphate ions and the unhydrated tricalcium aluminate grains (Kalousek and Benton, 1970; Mather, 1973; Soroka, 1980; Ogawa and Roy, 1981, 1982; Cohen, 1983b; Odler and Gasser, 1988; Brown and Taylor, 1999, Skalny et al., 2002). On the other hand, there were others who maintained it is the through-solution reaction which leads to expansive ettringite formation (Mehta, 1973; 1983; 2000; Mehta and Hu, 1978; Mehta and Wang, 1982; Ping and Beaudoin, 1992).

In the present paper two multi-field models will be developed to predict the sulphate induced degradation and expansion of cementitious composites:

one based on the topochemical reaction and one based on the through solution reaction of ettringite formation. The proposed models combine the state-of-the-art knowledge on chemistry of external sulphate attack with the transport of sulphate ions and the micromechanics of expanding ettringite inclusions leading to microcracking and structural degradation.

The main objective of this paper is to answer the basic question which of the two models of ettringite formation is more likely to produce the observed amount of macroscopic expansion of concrete specimens.

2 Mechanisms of external sulphate attack

Depending on the concentration of sulphate, composition of concrete, source and type of sulphate, the external sulphate attack on the field concrete may proceed in different ways and have different consequences for the structure durability (cf. Basista and Weglewski, 2008). For modelling purposes we shall focus here on the sulphate attack associated with ettringite and gypsum formation caused by the sodium sulphate (Na_2SO_4).

When the sodium sulphate is brought into contact with anhydrous particles of the hardened cement paste ettringite and gypsum may be produced which are responsible for concrete expansion and microcracking. This process is initiated by the reaction between the sodium sulphate and calcium hydroxide (CH)[1]:

$$Ca(OH)_2 + Na_2SO_4 + 2H_2O \rightarrow CaSO_4 \cdot 2H_2O + 2NaOH \qquad (1)$$

This is a through-solution reaction proceeding in the saqueous solution filling the pores of concrete. Calcium hydroxide when dissolved from the walls of pores reacts with the sodium sulphate from the ambient solution to form gypsum ($CaSO_4 \cdot 2H_2O$) and sodium oxide. It is commonly assumed that the volume difference between gypsum (reaction product) and $Ca(OH)_2$ (reactant) can be accommodated by the concrete porosity and the additional space released by the dissolved $Ca(OH)_2$. Consequently, a reasonable conclusion can be drawn that no expansion of the concrete specimen takes place at this stage of sulphate attack.

However, the chemical reaction proceeds further. The newly produced gypsum can react with some alumina-bearing phases like unhydrated tricalcium aluminate $3CaO \cdot Al_2O_3$ (C_3A) or hydrated calcium sulfoaluminate (monosulphate) to form ettringite, e.g.:

$$3CaO \cdot Al_2O_3 + 3(CaSO_4 \cdot 2H_2O) + 26H_2O \rightarrow 3CaO \cdot Al_2O_3 \cdot 3CaSO_4 \cdot 32H_2O$$

---
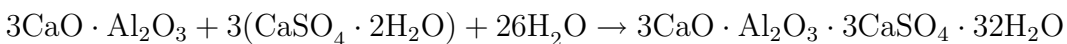
[1]abbreviated notation of the cement chemistry is used throughout the paper (cf. Table 1 in Appendix).

$$m : 270.2 + 3(172.1) + 26(18) \rightarrow 1254.5 \tag{2}$$

$$v : 88.8 + 3(74.1) + 26(18) \rightarrow 725.1$$

where m(g/mol) stands for the molar mass and v (cm^3/mol) for the molar volume of the reactants and the product.

As was mentioned earlier when reviewing the extensive literature on the sulphate attack research two competing chemical mechanisms of expansive ettringite formation can be distinguished: (1) topochemical and (2) through-solution mechanism. The topochemical, or solid-solid reaction, is a process in which atoms or ions create a new crystal directly on the surface of one of the reaction substrates, e.g. C_3A (Ping and Beaudoin, 1992). On the other hand, during the through-solution reaction all substrates are first dissolved in the water and the newly formed ettringite is then deposited on the pore walls. It should be stressed that depending on the environmental conditions, ettringite may crystallize in either type of reaction but not always the ettringite crystallization leads to cracking and expansion of concrete. The difference between these two types of reactions is also reflected in the way the pressure exerted by ettringite on the pore walls is computed. For ettringite produced in the topochemical reaction the crystallization pressure may be computed using micromechanical modelling but for ettringite created in a through-solution reaction equations derived from the chemical thermodynamics are usually used.

It seems that the topochemical scenario of the expansive ettringite formation is prevailing in the newest literature. For example, Skalny et al. (2002) postulate that the following conditions must be reached if ettringite crystallization is to lead to the expansion:

1. Volume of ettringite must exceed some threshold value which depends on the capillary porosity of concrete.

2. Only ettringite formed after the hydration of cement leads to the expansion. The volumetric expansion of ettringite formed during the hydration of cement (primary ettringite) can be accommodated by the elasticity of fresh cement paste – hence no expansion.

3. If sulphate attack leads to concrete expansion ettringite must be formed in a topochemical reaction.

A necessary prerequisite for the reaction between the sulphate ions and the C_3A grains to commence is that the suphate ions have to find their way to C_3A grains through a tortuous network of pores in the hardened concrete. It was reported by experimentalists that ettringite forms in capillary pores, occupying less than 50% of total concrete porosity, and does not form in gel

pores. The principal mechanism for transport through capillary pores is the diffusion driven by the sulphate concentration gradient. The exact kinetics of the reaction (2) in hardened concrete is generally not known. Consequently, both the first and the second order reactions were postulated for this purpose in the past (e.g. Krajcinovic et al., 1992; Gospodinov, et al., 1996; Tixier and Mobasher, 2003). We shall assume a second order reaction governed by the following kinetic equation (cf. Dawson, 1973)

$$\frac{dc_e}{dt} = k \, c \, c_a = k \, c \, \left(c_a^0 - c_e\right) \tag{3}$$

where k is the rate constant (reaction constant), c_e is the current (molar) concentration of ettringite, c is the current concentration of diffusing sulphate, c_a the current concentration of C$_3$A, c_a^0 is the initial concentration of C$_3$A in the hardened cement paste.

The assumption leading to equation (3) is supported by the observation that the damage of concrete depends only on the concentration of sulphates and C$_3$A but not on the content of calcium hydroxide (Biczok, 1972). The rate constant of the heterogeneous reaction (1)-(2) depends on the size, tortuosity and connectivity of the micropores. For external sulphate attack it is difficult to measure the rate constant, hence no credible experimental data for k were found in the literature. The values assumed by different authors vary from $1 \cdot 10^{-10} m^3/mol \cdot s$ to $1 \cdot 10^{-6} m^3/mol \cdot s$ (Tixier, 2000). In the absence of precise data, k is herein a parameter to be determined from phenomenological rather than microstructural considerations.

If gypsum is not in a solid state, the formation of ettringite from tricalcium aluminate via reaction (2) leads to the volume increase of 816% (Pommersheim and Clifton, 1994). This value is obtained from a simple calculation based on the molar volumes of solid reactants and the reaction product with account for the reaction stoichiometry: $\Delta V/V = v_e/v_a - 1 = 8.16$. However, this formula does not account for the advancement of the reaction and cannot thus be used to model expansion as a process in time. To compute the actual expansion caused by growing ettringite crystal one has to take into account the current concentrations of C$_3$A and ettringite obtained from the transport equation (non-steady diffusion) coupled with the reaction kinetics equation (3). The actual volumetric strain of growing ettringite crystal is then calculated from the following formula (Basista and Weglewski, 2008)

$$\varepsilon^{vc} = \frac{c_e \frac{\nu_e}{1-\phi_e} + c_a \nu_a}{c_a^0 \nu_a} - 1 \tag{4}$$

where $c_e(\mathbf{x}, t)$ is the actual concentration of ettringite, $c_a(\mathbf{x}, t)$ and $c_a^0(\mathbf{x}, t)$ are the actual concentration and initial concentration of tricalcium aluminate, re-

spectively, ν_e and ν_a are molar volumes of ettringite and tricalcium aluminate; ϕ_e is the porosity of ettringite.

If C$_3$A is the rate limiting reactant then at the reaction completion (i.e. for $c_a = 0$) we get

$$\varepsilon^{vc} = \frac{c_a^0 \frac{\nu_e}{1-\phi_e}}{c_a^0 \nu_a} - 1 = \frac{\nu_e}{(1 - \phi_e)\, \nu_a} - 1 = 8.96 \tag{5}$$

In Equation (5) the material balance of reactions (1)-(2) expressed in compounds concentrations was used leading to the relations $c_g = c_e = 3c_a^0$.

The initial unconfined growth of ettringite in the capillary pores has not been accounted for when calculating the volumetric strain (5). However, ettringite crystals must first fill in the empty space in capillary pores before they start exerting pressure on the pore walls. In other words, not all of the net volume increase will contribute to real expansion of the specimen and there will be a delay time (incubation period) for the macroscopic expansion to start. Following the work by Tixier and Mobasher (2003), we assume that the volumetric strain (5) is adjusted by a shift term depending on the total capillary porosity ϕ as follows

$$\varepsilon^v = \varepsilon^{vc} - b\phi \tag{6}$$

where b is the fraction of the capillary porosity filled in during the incubation period (not contributing to the volumetric strain).

3   Models of sulphate corrosion damage and expansion

The heterogeneous reactions (1-2) and the resulting crystallization of ettringite will take place at locations where C$_3$A grains are accessible for the diffusing sulphate ions. Despite the fact that the cement paste is modelled as a homogeneous elastic matrix the effective material will be quite complex comprising the elastic matrix, the expanding ettringite inclusions and the microcracks emanating from them.

If ettringite crystallizes from a supersaturated solution the pressure exerted by the ettringite crystal can be calculated using the equations of chemical thermodynamics. On the other hand, if ettringite crystals are formed through a topochemical reaction, the problem may be considered as an expanding inhomogeneous inclusion in an elastic microcracked matrix. Therefore, in the latter case the well established methods of micromechanics can be employed. The ettringite crystallization pressure is the driving force for microcracking of the surrounding hardened cement paste.

3.1 Crystallization pressure of ettringite formed from supersaturated solution

The main difference between the two models proposed in this paper consists in the way of calculation of the pressure exerted by the ettringite crystal. In the model where the ettringite precipitates from the supersaturated solution the chemical thermodynamics methodology is typically used for that purpose.

The chemical reaction of the ettringite formation can be written in the following form (Ping and Beaudoin, 1992)

$$\gamma_1 R_1 + \gamma_2 R_2 + \ldots + \gamma_N R_N \overset{\Delta G < 0}{\Longleftrightarrow} S \tag{7}$$
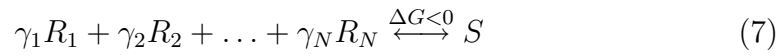
where R_i, i=1, 2, ... N is the ith reactant in the solution, γ_i is the stoichiometric coefficient of R_i, and S is the solid product of the reaction.

The reaction (7) can carry on spontaneously as long as the Gibbs free energy difference for this reaction is negative ($\Delta G < 0$). This condition can also be expressed as (Ping and Beaudoin, 1992)

$$A = \sum_{i=1}^{N} \gamma_i \mu_i - \mu_s > 0 \tag{8}$$

At the equilibrium state it becomes

$$\mu_s = \sum_{i=1}^{N} \gamma_i \mu_i \tag{9}$$

where: μ_i and μ_s are the chemical potentials of reactants R_i and solid product of the reaction (2) respectively; A is the chemical affinity of the reaction (2). During the sulphate attack, concentration of sulphate increases as well as the chemical potential of reactants. The only way to satisfy the equilibrium condition (9) is by an increase of the chemical potential of the solid product. Consequently, the following condition must hold (Ping and Beaudoin, 1992):

$$d\mu_s = \sum_{i=1}^{N} \gamma_i d\mu_i \tag{10}$$

Equation (10) indicates that if the chemical potentials of reactants increase due to any cause, the chemical potential of solid product will increase, too. If reaction (2) occurs in a confined space (a pore in a concrete matrix), the increase of the chemical potential of solid product will lead to an increase of the pressure exerted on the pore walls. The pressure can be derived from equation (10) using the expression for the chemical potential in function of

temperature (T) and pressure (p), (Ping and Beaudoin, 1992; Scherer, 1999; 2004):

$$d\mu_s = \left(\frac{\partial \mu_s}{\partial T}\right)_p dT + \left(\frac{\partial \mu_s}{\partial p}\right)_T dp = -\bar{s}_s dT + \bar{v}_s dp \tag{11}$$

where $\bar{s}_s$ and $\bar{v}_s$ are molar entropy and molar volume respectively. Chemical potential of reactants is described by following equation:

$$d\mu_i = d\mu_i^0(T, p_i) + (R \ln a_i)dT + RTd \ln a_i \tag{12}$$

where R is the universal gas constant and μ_i^0 is the chemical potential of R_i at standard state, a_i is the activity of R_i in the solution. Substitution of Equations (11) and (12) into (10) yields

$$\bar{v}_s dp = \sum_{i=1}^{N} \gamma_i d\mu_i^0(T, p_i) + (\bar{s}_s + R \sum_{i=1}^{N} \gamma_i d \ln a_i)dT + RT \sum_{i=1}^{N} \gamma_i d \ln a_i \tag{13}$$

Considering that the analysis is carried out for standard conditions of atmospheric pressure and constant temperature, and that pores are open, Equation (13) reduces to the following form

$$dp = \frac{RT}{\bar{v}_s} \sum_{i=1}^{N} \gamma_i d \ln a_i \tag{14}$$

It can be seen from Equation (14) that increase of the activity of any reactant in the pore solution will lead to an increase of the pressure of the confined solid product, in this case ettringite. Integration of equation (14) gives (Ping and Beaudoin, 1992; Scherer, 1999; 2004)

$$p_c = p_s - p_s^0 = \frac{RT}{\bar{v}_s} \ln \frac{K_{sp}}{K_{sp}^0} \approx \frac{RT}{\bar{v}_s} \ln \frac{c_e}{c_{e0}} \tag{15}$$

where $K_{sp} = \prod_{i=1}^{N} (a_i)^{\gamma_i}$ and $K_{sp}^0 = \prod_{i=1}^{N} (a_i^0)^{\gamma_i}$ are referred to as the solubility of solid product under pressure p_s and p_s^0 respectively, p_s^0 is the pressure of solid product without the interaction and is generally equal to the atmospheric pressure, c_e and c_{e0} are the actual and in "referred state" concentrations of ettringite. Equation (15) will be used to compute the ettringite crystallization pressure when ettringite is formed from the supersaturated solution. The ettringite crystallization pressure vs. the actual concentration of sulphates is depicted in Figure 1.
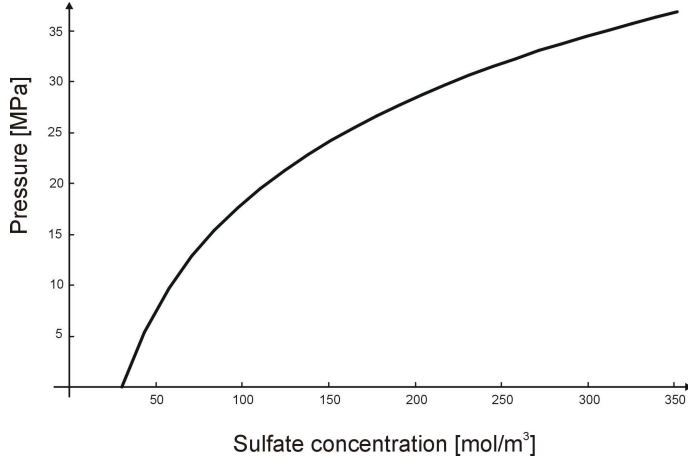
Figure 1: Ettringite crystallization pressure vs. sulphte concentration (through-solution model).

3.2 Crystallization pressure of ettringite formed in topo-chemical reaction

In case of the topochemical reaction the pressure exerted by the ettringite can be calculated using the formalism of micromechanics. The total eigenstrain within the ettringite crystal (inhomogeneous inclusion or inhomogeneity, cf. Mura, 1987) consists of two terms:

$$\varepsilon_{ij}^{**} = \varepsilon_{ij}^{*} + \varepsilon_{ij}^{eq} = \tfrac{1}{3}\varepsilon^{\mathrm{v}}\delta_{ij} + \varepsilon_{ij}^{eq} \tag{16}$$

where ε_{ij}^{*} is the inclusion eigenstrain (free expansion strain of the ettringite crystal) while ε_{ij}^{eq} is the equivalent eigenstrain resulting from disparity in the elastic moduli between the matrix and the inclusion.

In absence of external tractions the expression (16) takes the following closed form (Krajcinovic et al., 1992)

$$\varepsilon_{kk}^{**} = \frac{3\left(1-\nu\right)K^{*}}{\left(1+\nu\right)K^{*} - \left(4\nu-2\right)K}\varepsilon_{kk}^{*} = \beta(\omega)\,\varepsilon_{kk}^{*} \tag{17}$$

where the single star refers to the ettringite inclusion while the non-indexed moduli to the effective continuum. The $\beta(\omega)$ is formally introduced to account for the fact that ettringite inclusions grow in the microcracked matrix, the microcracking being quantified by the Budiansky-O'Connell (1976) crack density parameter $\omega = N < a^3 >$. Using the self-consistent estimates for the effective

elastic constants K and ν, the $\beta(\omega)$ becomes

$$\beta(\omega) = \frac{3\left[1 - \nu_0\left(1 - \frac{16}{9}\omega\right)\right]}{2\frac{E_0}{E^*}\left(1 - \frac{16}{9}\omega\right)(1 - 2\nu^*) + \left[1 + \nu_0\left(1 - \frac{16}{9}\omega\right)\right]} \tag{18}$$

The SCM estimates of the effective Young modulus E and the Poisson ratio ν used in Equation (18) have been linearized as $E \approx E_0\left(1 - 16/9\omega\right)$, $\nu \approx \nu_0\left(1 - 16/9\,\omega\right)$. The computations in Budiansky and O'Connell (1976) clearly indicate that for materials with Poisson's ratio in range of 0.1-0.3 (e.g. concrete) these approximations are quite accurate.

The expanding ettringite inclusion induces uniform radial pressure in the surrounding matrix. Only the normal component of pressure leads to crack propagation. It depends on the progress of the chemical reaction (2), which is indirectly recorded in ω, and is equal to (Basista and Weglewski, 2008)

$$p^n = \frac{2}{9}\frac{E(\omega)}{\nu(\omega) - 1}\varepsilon_{kk}^{**}(\omega) \tag{19}$$

3.3 Microcracking induced by ettringite crystallization pressure

The expanding ettringite crystal may cause microcracking of the hardened cement matrix. Assume that a penny-shaped crack (Fig. 2) nucleated in the matrix around the ettringite crystal as a result of the crystal growth pressure given by Equation (15) in case of the through-solution model, or by Equation (19) in case of the topochemical model. The mode-I stress intensity factor at the crack perimeter is derived to be (Basista and Weglewski, 2008)

$$K_I = \frac{2p^n}{\sqrt{\pi a}}\left(a - \sqrt{a^2 - r_{a0}^2}\right) \tag{20}$$

The penny-shaped microcrack under internal hydrostatic pressure shown in Figure 2 is stable since $\partial K_I/\partial a < 0$. In other words, as soon as the microcrack starts growing the crystallization pressure is released and an increase of ettringite coat thickness is needed to keep the microcrack growing. The critical microcrack radius is computed from the Griffith criterion $K_I = K_{Ic}$, where K_{Ic} is the fracture toughness of the hardened cement paste.

The critical values of ettringite crystallization pressure necessary to trigger the microcrack growth in the through-solution model are shown in Figure 3.
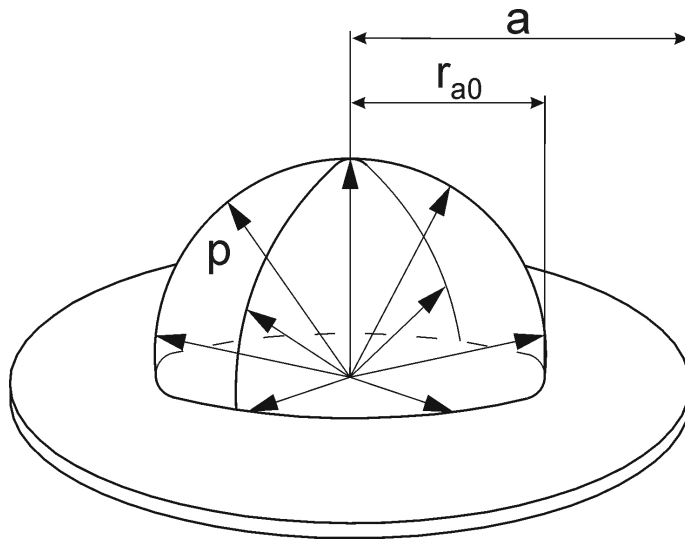
Figure 2: Penny-shaped microcrack under internal pressure of ettringite crystallization.

It is instructive to interpret the pressure vs. crack size curve in Figure 3 together with the pressure-concentration curve in Figure 1. For the sulphate concentration of 352 mol/m^3 used in the ASTM expansion test (cf. Section 4) the ettrinigte crystallization pressure equals ca. 35 MPa (cf. Fig.1). For such pressure level only microcracks with radius above 800 μm would start to grow, which contradicts the microscopic observations.
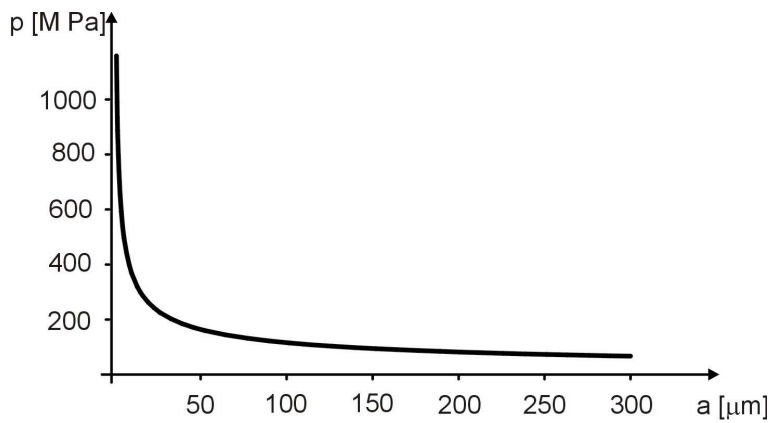

Figure 3: Microcrack growth pressure vs. crack radius (through-solution model)

3.4   Nonsteady diffusion with second-order reaction

Transport of sulphate ions through the porous hardened concrete is driven by
the concentration gradient and will be modelled as a symmetric 2D diffusion
problem. Let a prismatic specimen be initially saturated with chemically inert
water (to avoid moisture transport). At time $t = 0$ the specimen is immersed in
a solution with constant concentration of sulphates c_0 simulating the external
sulphate attack. The spatial and temporal distribution of sulphate ions in
the specimen is governed by a nonsteady diffusion-reaction equation (Fick's II
law):

$$\frac{\partial c}{\partial t} = \nabla \cdot (\mathbf{D}_{eff} \, \nabla c) + R(c, t) \tag{21}$$

In Equation (21) D_{eff} is the effective diffusivity tensor depending on the
microcracking, $R(c, t)$ is the reaction term (sink term) representing the rate
of sulphates consumption in the ettringite production calculated from mass
balance, i.e.

$$R(c) = \frac{dc^R}{dt} = -3\frac{dc_e}{dt} \tag{22}$$

where c^R is the molar concentration of Na_2SO_4 consumed in the first reaction
to produce the gypsum, c_e is the actual concentration of ettringite.

Combining Equations (22), (3) and (21) leads to a partial differential equation

$$\frac{\partial c}{\partial t} = \nabla \cdot (\mathbf{D}_{eff} \, \nabla c) - 3kc \left(c_a^0 - c_e \right) \tag{23}$$

where c_a^0 is the initial concentration of C_3A in the hardened cement paste, k
is the rate constant of chemical reaction. The concentrations of other active
substances can be determined from the stoichiometric analysis once the con-
centration of sulphates $c(\mathbf{x}, t)$ is computed solving the initial boundary value
problem. Note that the double decomposition reactions (1-2) can be termi-
nated either by discontinuing the supply of the sulphates before all C_3A is
consumed ($c = 0$), or when the entire supply of C_3A has been exhausted
rendering the specimen chemically inert to further sulphate attack ($c_a^0 = c_e$).

3.5   Effective transport properties.

It is reasonable to assume that tricalcium aluminate grains are distributed
randomly within the hardened cement paste. Therefore, if no external forces
act on the corroding structural element the ettringite induced damage will be
isotropic. However, the dependence of the diffusivity on the randomly nu-
cleating microcracks should be studied in two consecutive regimes: (i) the
distributed microcracking regime, and (ii) the percolation regime. Despite

that damage mechanics and percolation theory differ fundamentally in modelling microcracking phenomena and refer to different microcracks densities regimes, both approaches employ the same Budiansky-O'Connell parameter ω to quantify the evolving material deterioration (Basista, 2001). Two different percolation thresholds should be distinguished: $\omega = \omega_c$ - conduction percolation threshold at which a spanning cluster traverses the volume creating a worm-hole (percolation front), and $\omega = \omega_{ec}$ - elastic or rigidity percolation threshold at which a cluster of cracks transects the volume (fracture front) making the elastic modulus vanish and the diffusion practically instantaneous.

The diffusion through the matrix containing penny-shaped microcracks and the percolation through the spanning cluster of microcracks will be modelled as a parallel connection of the two transport phenomena (Krajcinovic et al., 1992):

$$D_{eff} = D_0 \left(1 + \frac{32}{9}\omega\right) + D_p \tag{24}$$

where the first term is the SCM solution (Salganik, 1974) while D_p denotes the percolation term defined as follows:

$$D_p = D_0 \frac{(\omega - \omega_c)^2}{\omega_{ec} - \omega} \quad for \quad \omega_c < \omega < \omega_{ec}$$

$$D_p = 0 \quad for \quad \omega < \omega_c$$

$$D_p = \infty \quad for \quad \omega > \omega_{ec} \tag{25}$$

The diffusivity D_0 of virgin (undamaged) material depends on the initial porosity ϕ of concrete, and can be expressed as follows (Garboczi and Bentz, 1992)

$$\frac{D_0}{D^\mu} = 0.001 + 0.07\,\phi^2 + H(\phi - 0.18)\,1.8\,(\phi - 0.18)^2 \tag{26}$$

where H is the Heaviside function, D^μ is the diffusion coefficient of the ionic species in free solution. The initial porosity depends on w/c ratio according to the following formula (Marchand et al., 2002)

$$\phi = 1 - \frac{1 + 1.31\,\alpha}{1 + 3.2\,w/c} \tag{27}$$

where α is the degree of hydration of cement.

The conduction percolation threshold ω_c for randomly distributed equisized penny-shaped was determined by numerical simulations in Charlaix (1986) as $\omega_c = N_c a^3 \approx 0.182$, where N_c is the critical number of cracks per unit volume forming a cluster connecting the opposite sides of the specimen. The rigidity percolation threshold was determined in Sornette (1988) as $\omega_{ec} =$

$\langle N \, a^3 \rangle_c \approx 0.712$. The critical exponent in Equation $(25)_1$ equals 2 as deduced from the considerations in Stauffer (1985) on the scaling law for the diffusivity attributable to spanning cluster.

In case of the effective elastic moduli the SCM estimates in Equation (18) are valid for small to moderate densities of microcracks. When microcracks clusters start to emerge ($\omega > \omega_c$) the proposed approach switches to the percolation model (Basista, 2001).

3.6   Stress-strain relation.

The macrostrains are related to the macrostresses as (Mura, 1987)

$$\boldsymbol{\varepsilon} = \mathbf{S}\left(\omega\right) : \boldsymbol{\sigma} + f\,\boldsymbol{\varepsilon}^{**} \tag{28}$$

where $\mathbf{S}(\omega)$ is the effective compliance tensor accounting for the ettringite induced microcracking, f is volume density of ettringite inclusions, $\boldsymbol{\varepsilon}^{**}$ the total eigenstrain tensor defined in Equation (17), σ is the stress induced by the nonlinear profile of sulphate concentration in the elastic matrix. The components of $\mathbf{S}(\omega)$ can be computed using e.g. the SCM estimates for the effective Young modulus and the Poisson ratio.

To make use of Equation (28) it is necessary to relate the concentration of sulphates $c(\mathbf{x}, t)$ obtained from the solution of diffusion-reaction Equation (23) and the damage parameter $\omega(\mathbf{x}, t)$. First, the molar concentration of sulphates consumed to form ettringite crystals $c^R(\mathbf{x}, t)$ is determined by integration of the reaction kinetic equation (3), i.e.

$$c^R\left(\mathbf{x}, t\right) = 3c_e\left(\mathbf{x}, t\right) = 3c_a^0 \left[1 - \exp\left(-k \int_0^1 c\left(\mathbf{x}, t\right) dt\right)\right] \tag{29}$$

When $c^R(\mathbf{x}, t)$ is known, the current concentrations of ettringite, tricalcium aluminate and gypsum $c_e(\mathbf{x}, t)$, $c_a(\mathbf{x}, t)$, $c_g(\mathbf{x}, t)$ are known, too. Hence, it is possible to determine the volumetric strain from Equation (4), the inhomogeneity eigenstrain from Equation (17) and the crystallization pressure from Equation (15) for the through-solution reaction or (19) for the topochemical one. The microcrack density parameter ω is computed at each time step, the microcrack radius being obtained from $K_I = K_{Ic}$ criterion. In addition to the equations listed so far the governing set involves the equilibrium equations, compatibility and the boundary conditions for a particular initial boundary-value problem.

4 Application

Consider a slender mortar prism (ASTM C490 specimen) immersed in sodium sulphate solution of concentration 0.352 mol/l (Figure 4). It is a symmetric initial boundary-value problem with two-dimensional diffusion and plane cross sections assumed. The normal expansion strain in axial direction is the primary mode of deformation. The diffusion of sulphates from the axial direction is neglected. The nonsteady diffusion-reaction Equation (23) in the plane case
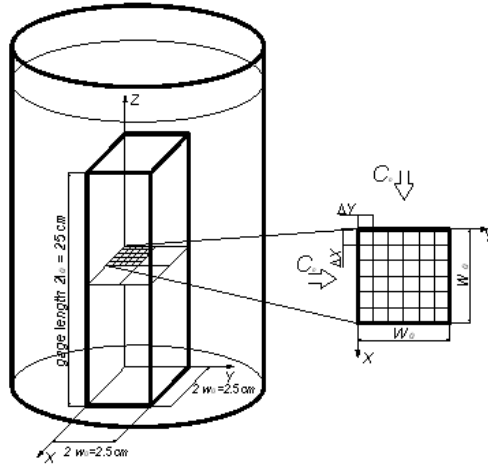

Figure 4: ASTM test specimen to measure axial expansion of mortar in external sulphate attack.

becomes

$$\frac{\partial \tilde{c}}{\partial \tilde{t}} = \frac{\partial}{\partial \tilde{x}} \left\{ \left[\tilde{D}_0 \left(1 + \tfrac{32}{9}\omega \right) + D_p \right] \frac{\partial \tilde{c}}{\partial \tilde{x}} \right\} +$$

$$\frac{\partial}{\partial \tilde{y}} \left\{ \left[\tilde{D}_0 \left(1 + \tfrac{32}{9}\omega \right) + D_p \right] \frac{\partial \tilde{c}}{\partial \tilde{y}} \right\} - 3\tilde{k}\tilde{c} \left(\tilde{c}_a^0 - \tilde{c}_e \right) \tag{30}$$

The non-dimensional quantities in Equation (30) are defined as:

$$\tilde{x} = x/w_0, \quad \tilde{c} = c/c_0, \quad \tilde{c}_e = c_e/c_0, \quad \tilde{c}^R = c^R/c_0, \quad \tilde{t} = t/T, \quad \tilde{D}_0 = \frac{D_0 T}{w_0^2}$$

where $T = 24$ hours.

To solve Equation (30) the FEM was used and a source code was worked out. The discretized form of Equation (30) reads

$$\mathbf{C}\frac{\mathbf{c}^{n+1} - \mathbf{c}^n}{\Delta t} = -\tilde{D}_{eff}\,\mathbf{K}\,\mathbf{c}^n - 3\tilde{k}\left(\tilde{c}_a^0 - \tilde{c}_e\right)\,\mathbf{C}\,\mathbf{c}^n \qquad (31)$$

where $\mathbf{C}$ and $\mathbf{K}$ are capacitance and stiffness matrix respectively; $\mathbf{c}^n$ is the known vector computed in the previous time step or given by the initial condition, $\mathbf{c}^{n+1}$ is the unknown vector of the actual sulphate concentration inside the concrete specimen. Matrices $\mathbf{C}$ and $\mathbf{K}$ were obtained using Galerkin approximation and square, four node elements. For time discretization the forward finite difference approximation was used.

The stress consistency conditions for a 2D nonsteady diffusion problem can be expressed as

$$\frac{\partial^2}{\partial\tilde{x}\partial\tilde{y}}\left[\sigma\left(\tilde{x},\tilde{y},\tilde{t}\right) + E\left(\tilde{x},\tilde{y},\tilde{t}\right)\,f\left(\tilde{x},\tilde{y},\tilde{t}\right)\,\varepsilon^{**}\left(\tilde{x},\tilde{y},\tilde{t}\right)\right] = 0 \qquad (32)$$

Finally, the axial strain due to the diffusion in x and y directions is

$$\varepsilon(\tilde{x},\tilde{y},\tilde{t}) = \frac{1}{E(\tilde{x},\tilde{y},\tilde{t})}\int_0^1\int_0^1 \varepsilon^{**}(\tilde{x},\tilde{y},\tilde{t})\,E(\tilde{x},\tilde{y},\tilde{t})\,f(\tilde{x},\tilde{y},\tilde{t})\,d\tilde{x}\,d\tilde{y} \quad for \quad \omega < \omega_c \qquad (33)$$

and for the heavily damaged region:

$$\varepsilon(\tilde{x},\tilde{y},\tilde{t}) = f\,\varepsilon^{**} \quad for \quad \omega > \omega_c \qquad (34)$$

Due to the problem symmetry only one fourth of the cross section was considered as shown in Figure 4.

The main outcome of the proposed models i.e. the specimen expansion vs. time of contact with the sulphate solution are presented in Figure 5 (through-solution model) and Figure 6 (topochemical model) for different values of C_3A content. The material parameters used in the computations are: $D^\mu = 0.5 \cdot 10^{-10}\,\mathrm{m}^2/\mathrm{s}$, $\phi_e = 0.18$, $b=0.5$, $c_0 = 352\mathrm{mol/m}^3$, $c_{e0} = 30\mathrm{mol/m}^3$, $r_{a0} = 1\mu\mathrm{m}$, $f_g = 6\%$, $E_0 = 20\mathrm{GPa}$, $E_e = E_0/6$, $\nu_0 = 0.3$, $\nu_e = 0.2$, $K_{Ic} = 0.8\mathrm{MPa}\sqrt{\mathrm{m}}$, k $= 0.9 \cdot 10^{-10}\mathrm{m}^3/\mathrm{mol/s}$. The initial and boundary conditions were $c(x,y,0) = 0$, $c(0,0,t) = c(2w_0, 2w_0, t) = c_0$. As no precise experimental value was available for the rate constant from experiments in field or laboratory conditions, k is a fitting parameter of the model. Its numerical value was estimated by fitting the 4.3% C_3A expansion curve. The comparison of the Ouyang test data with the present model predictions for the 8.8% and 12% of C_3A contents is shown in Figure 5 for a through-solution reaction and in Figure 6 for the topochemical reaction.
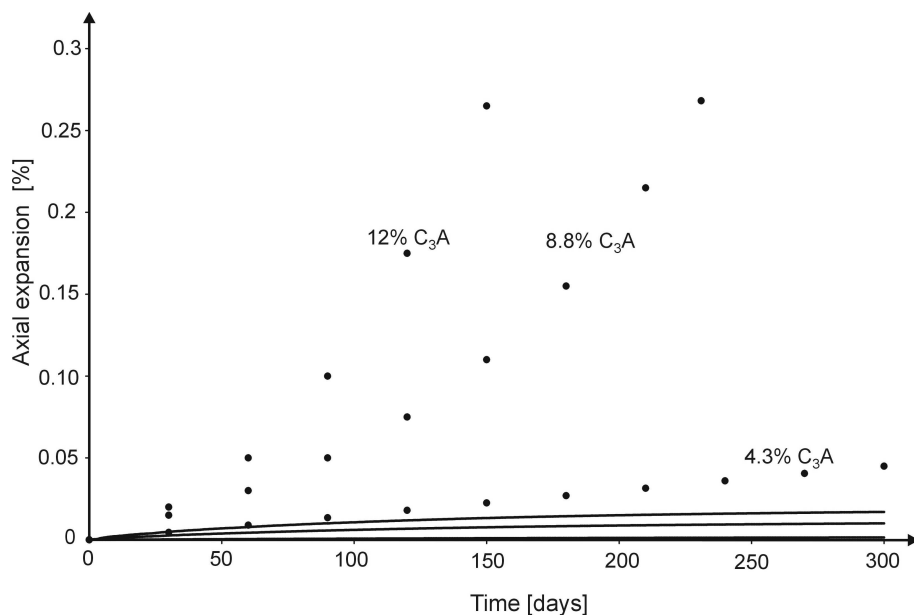
Figure 5: Expansion of mortar specimen due to uptake of sulphate ions. Solid lines - predictions of the present model based on the through-solution reaction, circles - test data by Ouyang et al. (1988).
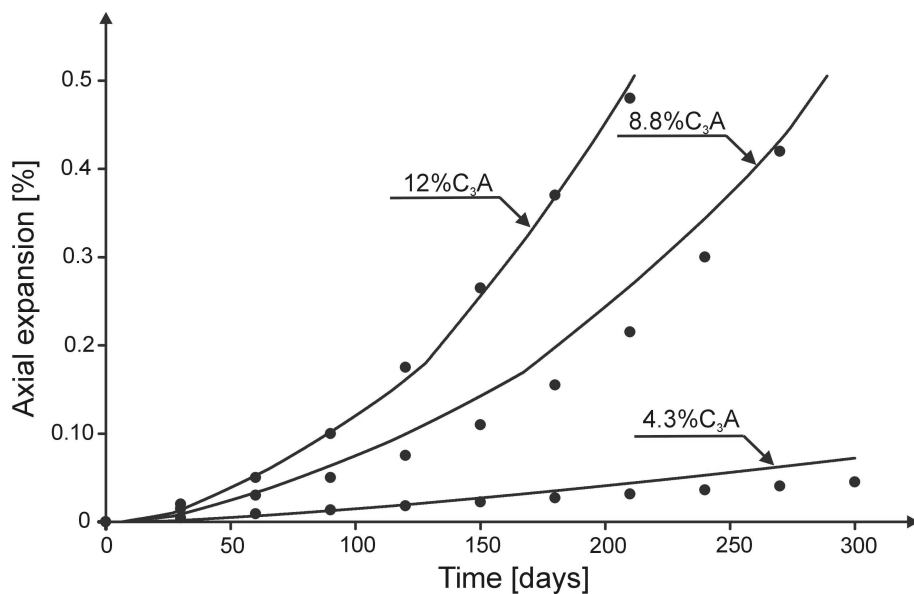

Figure 6: Expansion of mortar specimen due to uptake of sulphate ions. Solid lines - predictions of the present model based on the topochemical reaction, circles - test data by Ouyang et al. (1988).

5   Summary and conclusions

Two models have been proposed for the progressive damage in hardened concrete induced by the external sulphate attack based on different chemical mechanism of expansive ettringite formation (through-solution vs. topochemical). Both of them combine transport of sulphate ions, the stress and strain fields due to expanding inhomogeneities (ettringite crystals), the microcracking of elastic matrix and the percolation. The governing equations of the models have been implemented numerically using the *FEM* and applied to predict expansions of mortar specimens exposed to constant concentration of sulphates.

The predicted axial expansions of the ASTM specimen were compared with the experimental data of Ouyang et al. (1988). This comparison leads to following conclusions:

- the pressure of expanding ettringite formed in the topochemical reaction may cause nucleation and propagation of microcracks in the hardended cement paste,

- the topochemical model is capable of correct predictions of the macroexpansion both qualitatively and quantitatively (Fig. 6),

- pressure generated in a through-solution reaction is insufficient to cause microcrack nucleation and growth (cf. Figs. 1 and 4), thus no reasonable values of axial expansion are predicted by this model (Fig. 5).

References

[1] Basista, M. (2001). *Micromechanical and Lattice Modeling of Brittle Damage*, IFTR Reports, Warsaw.

[2] Basista, M., Weglewski, W. (2008). Chemically-assisted damage of concrete: a model of expansion under external sulphate attack, *International Journal of Damage Mechanics*, (in press)

[3] Biczok, I. (1972). *Concrete Corrosion Concrete Protection*, Akademiai Kiado, Budapest.

[4] Brown, P.W. and Hooton, R.D. (2002). Ettringite and thaumasite formation in laboratory concretes prepared using sulphate-resisting cements, *Cement and Concrete Composites*, **24**: 361-370.

[5] Brown, P.W. and Taylor, H.F.W. (1999). The role of ettringite in external sulphate attack, In: Marchand J., Skalny, J., (eds), *Materials Science of Concrete Special Volume: Sulphate Attack Mechanisms*, The American Ceramic Society, Westerville, OH, pp. 73-98.

[6] Budiansky, B. and O'Connell, R.J. (1976). Elastic moduli of cracked solid, *International Journal of Solids and Structures*, **12**: 81-97.

[7] Charlaix, E. (1986). Percolation thresholds of a random array of discs: A numerical simulation, *Journal of Physics A*, **19**: L533-L536.

[8] Cohen, M.D. (1983a). Theories of expansion in sulfoaluminate-type expansive cements: Schools of thought, *Cement and Concrete Research*, **13**: 809-818.

[9] Cohen, M.D. (1983b). Modelling of expansive cement, *Cement and Concrete Research*, **13**: 519-528.

[10] Cohen, M.D. and Bentur, A. (1988). Durability of Portland cement-silica fume pastes in magnesium sulphate and sodium sulphate solutions, *ACI Materials Journal*, **85**: 148-157.

[11] Cohen, M.D. and Mather, B. (1991). Sulphate attack on concrete – research needs, *ACI Materials Journal* **88**: 62-69.

[12] Dawson, B.E. (1973). *Kinetics and Mechanisms of Reactions*, Methuen Educational Ltd., London

[13] Garboczi E.J. and Bentz, D.P. (1992). Computer stimulation of the diffusivity of cement-based materials, *Journal of Material Sciences*, **27**: 2083-2092

[14] Gospodinov, P., Kazandijev, R. and Mironova, M. (1996). Effect of sulphate diffusion on the structure of cement stone, *Cement and Concrete Composites*, **18**: 401-407.

[15] Kalousek, G.W., Benton, E.J. (1970). Mechanism of sea water attack on cement pastes, ACI J. **67**, 187-192.

[16] Krajcinovic, D., Basista, M., Mallick, K. and Sumarac, D. (1992). Chemo-micromechanics of brittle solids, *Journal of the Mechanics and Physics of Solids*, **40**: 965-990.

[17] Kuhn, D., Bangert, F. and Meschke, G. (2004). Coupled chemo-mechanical deterioration of cementitious composites. Part I, II, *International Journal of Solids and Structures*, **41**: 15-67

[18] Lea, F.M. (1998). *Lea's Chemistry of Cement and Concrete.* 4th Edition, Edward Arnold, London.

[19] Marchand, J. (2001). Modeling the behavior of unsaturated cement systems exposed to aggressive chemical environments. *Matériaux et Constructions*, **34**: 195-200.

[20] Marchand, J., and Skalny, J. (eds), (1999). *Materials Science of Concrete Special Volume: Sulphate Attack Mechanism*s, The American Ceramic Society, Westerville, OH.

[21] Marchand, J., Samson, E., Malrais, Y., Beaudoin, J.J. (2002). Theoretical analysis of the effect of weak sodium sulfate solutions on the durability of concrete, *Cement and Concrete Composites*, **24**: 317-329.

[22] Mather, B. (1973). A discussion of the paper "Mechanisms of expansion associated with ettringite formation" by P.K. Mehta. *Cement and Concrete Research,* **3**: 651-652.

[23] Mehta, P.K. (1973). Mechanism of expansion associated with ettringite formation, *Cement and Concrete Research*, **3**:1-6.

[24] Mehta, P.K. (1983). Mechanism of sulphate attack on Portland cement concrete – another look, *Cement and Concrete Research*, **13**: 401-406.

[25] Mehta, P.K. (2000). Sulphate attack on concrete: Separating the myth from reality. *Concrete International*, **22**: 57-61.

[26] Mehta, P.K. and Hu, F. (1978). Further evidence for expansion of ettringite by water absorption, *Journal of the American ceramic Society*, **61**: 179-181.

[27] Mehta, P.K.and Monteiro, P.J.M. (1993). *Concrete: Structure, Properties and Materials*, McGraw-Hill, New York.

[28] Mehta, P.K. and Wang, S. (1982). Expansion of ettringite by water absorption, *Cement and Concrete Research*, 12: 121-122.

[29] Mironova, M.K., Gospodinov, P.N. and Kazandijew, R.F. (2002). The effect of liquid push out of the material capillaries under sulphate ion diffusion in cement composites, *Cement and Concrete Research*, **32**: 9-15.

[30] Moukwa, M. (1990). Characteristics of the attack of cement paste by $MgSO_4$ and $MgCl_2$, *Cement and Concrete Research*, **20**: 148-158.

[31] Mura, T. (1987). *Micromechanics of Defects in Solids*, Martinus Nijhoff Publ., The Hague, The Netherlands.

[32] Odler, I. and Gasser, M. (1988). Mechanism of sulphate expansion in hydrated Portland cement, *Journal of the American Ceramic Society*, **71**: 1015-1020.

[33] Ogawa, K. and Roy, D.M. (1981) .$C_4A_3\bar{S}$ hydration, ettringite formation and its expansion mechanism I, *Cement and Concrete Research*, **11**: 741-750.

[34] Ogawa, K. and Roy, D.M. (1982). $C_4A_3\bar{S}$ hydration, ettringite formation and its expansion mechanism II. *Cement and Concrete Research*, **12**: 101-109.

[35] Ouyang, C., Nanni, A. and Chang, W.F. (1988). Internal and external sources of sulphate ions in portland cement mortar: two types of chemical attack, *Cement and Concrete Research*, **18**: 699-709.

[36] Ping, X. and Beaudoin, J.J. (1992). Mechanism of sulphate expansion, Part I and II, *Cement and Concrete Research*, **22**: 631-640 and 845-854.

[37] Pommersheim, J. and Chang, J. (1988). Kinetics of hydration of tricalcium aluminate in the presence of gypsum, *Cement and Concrete Research*, **18**: 911-922.

[38] Pommersheim, J. and Clifton, J.R. (1994). Sulphate attack of cementitious materials: volumetric relations and expansion, NISTIR 5390, *National Institute of Standards and Technology*, Gaithersburg, MD, 1-19.

[39] Saetta, A., Schrefler, B. and Vitaliani, R. (1993). The carbonation of concrete and the mechanisms of moisture, heat and carbon dioxide flow through porous materials, *Cement and Concrete Research*, 23: 761-772.

[40] Saetta, A., Scotta, R. and Vitaliani, R. (1998). Mechanical behavior of concrete under physical-chemical attacks, *ASCE Journal of Engineering Mechanics*, **124**: 1100-1109.

[41] Salganik, R.L. (1974). Transfer processes in bodies with a great number of cracks, *Mechanics of Solids (Inzhenerno-Fizicheskij Zhurnal)*, **27**: 1069-1075.

[42] Samson, E., Marchand, J. and Beaudoin, J.J. (2000). Modeling the influence of chemical reactions on the mechanisms of ionic transport in porous materials. An overview, *Cement and Concrete Research*, **30**: 1895-1902.

[43] Santhanam, M., Cohen, M.D. and Olek, J. (2001). Sulphate attack research – whiter now?, *Cement and Concrete Research*, **31**: 845-851.

[44] Scherer, G.W. (1999). Crystallization in pores, *Cement and Concrete Research*, **29**: 1347-1358

[45] Scherer, G.W. (2004). Stress from crystallization of salt, *Cement and Concrete Research*, **34**: 1613-24

[46] Skalny, J., Marchand, J. and Odler, I. (2002). *Sulphate Attack on Concrete*, Spon Press, London.

[47] Snyder, K.A., Clifton, J.R. (1995). 4SIGHT: A computer program for modeling degradation of underground low level concrete vaults, NISTIR 5612, *National Institute of Standards and Technology*, Gaithersburg, MD.

[48] Sornette, D. (1988). Critical transport and failure in continuum crack percolation, *Journal de Physique. France*, **49**: 1365-1377.

[49] Soroka, I. (1980). *Portland Cement Paste and Concrete*, Chemical, New York.

[50] Stauffer, D. (1985). *Introduction to Percolation Theory*, Taylor & Francis, London, UK.

[51] Tixier, R. (2000). Microstructural development and sulphate attack modeling in blended cement-based materials, *PhD Dissertation*, Arizona State University, Tempe, AZ.

[52] Tixier, R. and Mobasher, B. (2003). Modeling of damage in cement-based materials subjected to external sulphate attack I, II, *ASCE Journal of Materials in Civil Engineering*, **15**: 305-322.

Appendix

Compound	Mineralogical name	Chemical formula	Cement chemistry abbreviation
Calcium hydroxide	portlandite	$Ca\,(OH)_2$	CH
Calcium silicate hydrate	-	$x\,CaO \cdot SiO_2 \cdot y\,H_2O$	C-S-H
Tricalcium aluminate	-	$Ca_3Al_2O_6$	C_3A
Magnesium hydroxide	brucite	$Mg(OH)_2$	MH
Sodium sulphate	-	Na_2SO_4	$N\bar{S}$
Calcium sulphate dihydrate	gypsum	$CaSO_4 \cdot 2H_2O$	$C\bar{S}H_2$
Monosulphate	-	$Ca_4Al_2(OH)_{12} \cdot SO_4 6H_2O$	$C_4A\bar{S}H_{12}$
Calcium sulfoaluminate	ettringite	$3CaO \cdot Al_2O_3 \cdot 3CaSO_4 \cdot 32H_2O$	$C_6A\bar{S}_3H_{32}$

Table 1: Compounds of primary interest in sulphate attack on concrete: cement chemistry notation

where: $C=CaO$, $S=SiO_2$, $A=Al_2O_3$, $M=MgO$, $N=Na_2O$, $H=H_2O$, $\bar{S}=SO_3$, $\bar{C} = CO_2$.

Mikromehaničko modeliranje sulfatne korozije u betonu: uticaj reakcije formiranja etringita

Razvijena su dva mikromehanička modela za simulaciju širenja cementnih kompozita izloženih spoljašnjem sulfatnom napadu. Razlika izmedju modela leži u formi etringitne formacije (kroz topohemijsko rešenje). U oba slučaja se predpostavlja da Fikov drugi zakon rukovodi transport sulfatnih jona. Ešelbijevo rešenje i metod ekvivalentnog uključka se koriste za odredjivanje rezidualne deformacije širećih etringitnih kristala u mikronaprsnutoj otvrdnutoj cementnoj pasti. Degradacija transportnih osobina se proučava u efektivnoj sredini i perkolacionom režimu. Dvodimenzioni početno-granični problem širenja betonske epruvete potopljene u mešavinu sodium sulfata se rešava i uporedjuje sa raspoloživim eksperimentalnim podacima. Dobijeni rezultati ukazuju da je topohemijski mehanizam u stanju da proizvede eksperimentalno uočeni iznos širenja.